Supporting information

Surface Crystallization of Ionic Liquid Crystals

Mónia A. R. Martins,[abc] Pedro J. Carvalho,[a] Douglas Alves,[d] Claudio Dariva,[d] Mariana C. Costa,[e] Rute A. S. Ferreira,[f] Paulo S. André,[g] Pedro Morgado,[h] Simão P. Pinho,[bc] Eduardo J. M. Filipe[h] and João A. P. Coutinho*[a]

[a.] CICECO, Department of Chemistry, Univ. Aveiro, Portugal

[b.] Associate Laboratory LSRE-LCM, Polytechnic Institute of Bragança, Portugal

[c.] CIMO - Mountain Research Center, Polytechnic Institute of Bragança, Portugal

[d.] Institute of Research and Technology, UNIT, Brazil

[e.] School of Chemical Engineering, Univ. of Campinas, Brazil

[f.] CICECO, Department of Physics, Univ. Aveiro, Portugal

[g.] Instituto de Telecomunicações and Department of Electronic and Computer Engineering, IST – Univ. of Lisbon, Portugal

[h.] Centro de Química Estrutural, IST – Univ. of Lisbon, Portugal

Corresponding Author: jcoutinho@ua.pt

Differential Scanning Calorimetry (DSC)

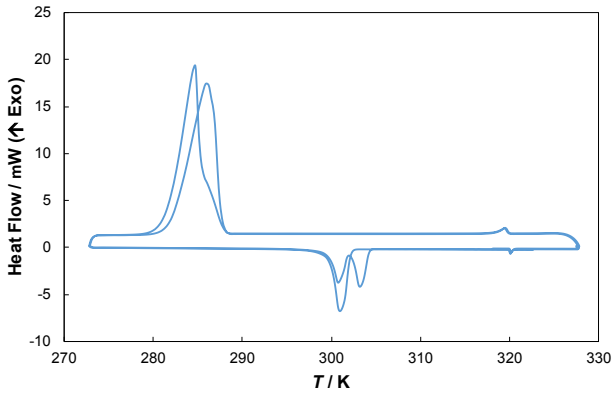

Figure S1. DSC thermogram displaying the reversible crystal – crystal transitions of 1-dodecyl-3-methylimidazolium tetrafluoroborate (heating and cooling rate: 1 K·min^{-1} and 2 K·min^{-1}, respectively). Exothermic peaks (↑) correspond to crystallization while endothermic peaks (↓) to melting.

Density and Viscosity

Table S1. Experimental densities, ρ, and viscosities, η, of the pure ILC as a function of temperature, at 0.1 MPa.

T / K	ρ / g·cm^{-3}	T / K	η / mPa·s^{-1}
	$[C_{12}C_1im][BF_4]$[a]		$[C_{12}C_1im][BF_4]$[b]
303.16	1.04565	319.75	385.83
308.14	1.04226	319.85	383.16
313.14	1.03887	319.95	380.64
318.14	1.03551	320.05	377.97
323.14	1.03231	320.15	375.73
328.14	1.02900	321.15	351.02
333.14	1.02568	322.15	328.10
338.14	1.02238	323.15	309.63
343.14	1.01908	333.15	171.98
348.14	1.01579	343.15	103.54
353.14	1.01253	353.15	66.61
358.14	1.00927	363.15	45.24
363.14	1.00603	373.15	32.10

[a] Experimental values; standard uncertainties, u, are $u(\rho) = \pm 5{\cdot}10^{-5}$ g·cm^{-3}, $u(T) = 0.01$ K and $u_r(p) = 0.05$; [b] Experimental values; standard uncertainties, u, are $u_r(\eta) = 0.35\%$, $u(T) = 0.02$ K and $u_r(p) = 0.05$.

The experimental density data was further correlated according to a linear dependency on the temperature:

$$ln\rho = A_0 + A_1 T \quad \text{(S1)}$$

where ρ is the density, and A_0 and A_1 are fitting parameters. The isobaric thermal expansion coefficient, α_p, which considers the volumetric changes with temperature, was then derived from equation S1 (no temperature dependence was assigned to this property):

$$\alpha_p = -\frac{1}{\rho}\left(\frac{\partial \rho}{\partial T}\right)_p = -\left(\frac{\partial ln\rho}{\partial T}\right)_p = -A_1 \quad \text{(S2)}$$

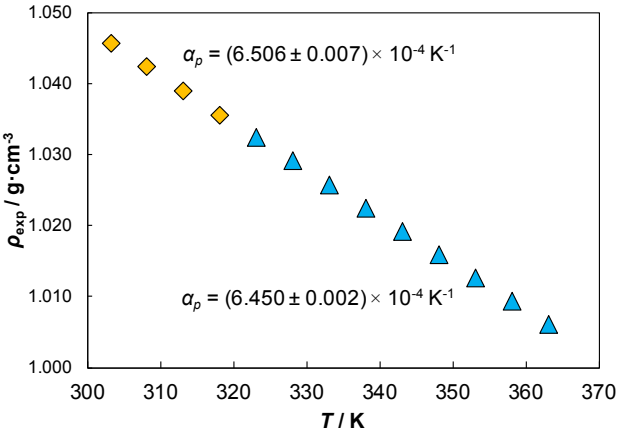

Figure S2. Experimental densities of $[C_{12}C_1im][BF_4]$ and thermal expansion coefficients in the liquid crystal (yellow diamonds) and clear liquid (blue triangles) phases.

The viscosity was correlated using the Vogel–Tammann–Fulcher (VTF) model[1] – equation S3 – and the energy barrier (E) estimated based on the viscosity dependence with temperature[2] using equation S4. Results at different temperatures are presented in Figure S3.

$$\eta(T) = A_\eta exp\left[\frac{B_\eta}{T - C_\eta}\right] \quad \text{(S3)}$$

$$E = R\frac{\partial(ln[\eta(T)])}{\partial(1/T)} \quad \text{(S4)}$$

where A_η, B_η, and C_η are adjustable parameters estimated from experimental data.

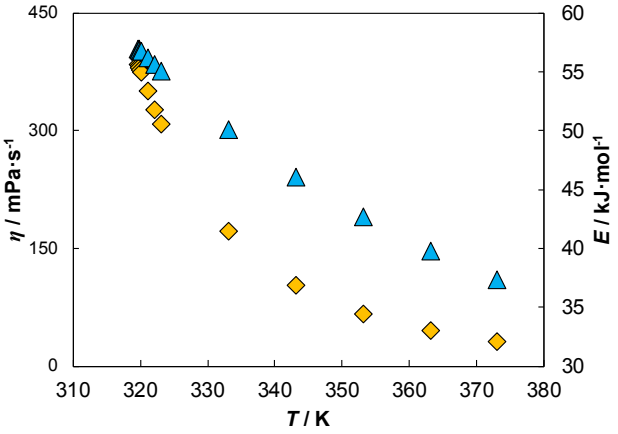

Figure S3. Experimental viscosity (yellow diamonds) and energy barrier (blue triangles) of $[C_{12}C_1im][BF_4]$ as function of temperature.

Refractive Index

Table S2. Refractive Index value, n_D, of the studied ILC as function of temperature and at atmospheric pressure.

T / K	n_D[a]	T / K	n_D[a]
308.15	1.4455	319.95	1.4340
311.15	1.4444	320.15	1.4339
312.15	1.4441	322.15	1.4333
314.15	1.4433	323.15	1.4329
316.15	1.4425	323.15	1.4329
317.15	1.4421	324.15	1.4326
318.15	1.4417	324.15	1.4326
319.15	1.4412	324.15	1.4326
319.65	1.4410	325.15	1.4323
319.75	1.4341	325.15	1.4322
319.85	1.4340	321.15	1.4333

[a] Experimental values; standard uncertainties, u, are $u(n_D) = \pm 2 \cdot 10^{-5}$ g·cm^{-3}, $u(T) = \pm 0.01$ K and $u_r(p) = 0.05$.

Spectroscopic Ellipsometry

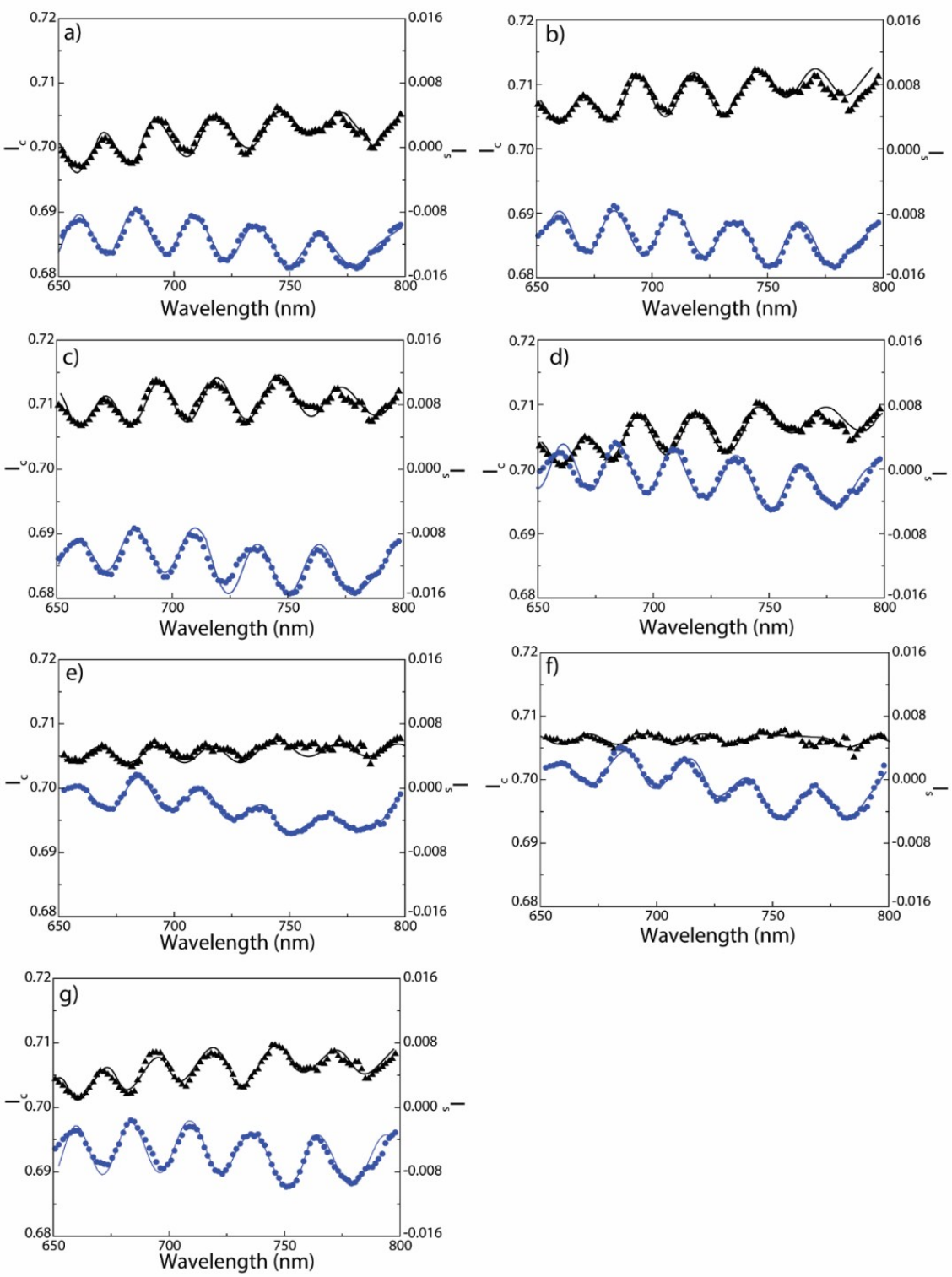

Figure S4. Ellipsometric parameters I_c (black triangles) and I_s (blue circles) measured for the $[C_{12}C_1im][BF_4]$ ILC with a temperature of a) 299.15 K, b) 315.05 K, c) 320.25 K, d) 320.85 K, e) 322.15 K, f) 325.25 K and g) 330.95 K; the lines represent the best data fit (r^2>0.9).

Table S3. Ellipsometric fitting parameters *A*, *B* and *C* (equation 3) at different temperatures.

T / K	*A*	*B* (× 10^3 nm^2)	*C* (× 10^8 nm^4)
299.15	1.440 ± 0.002	0.21 ± 0.09	6.827 ± 0.001
315.05	1.436 ± 0.001	0.21 ± 0.01	6.843 ± 0.001
320.25	1.434 ± 0.001	0.27 ± 0.01	6.413 ± 0.002
320.85	1.424 ± 0.001	2.05 ± 0.04	3.426 ± 0.009
322.15	1.424 ± 0.002	1.55 ± 0.03	3.782 ± 0.004
325.25	1.424 ± 0.001	1.48 ± 0.03	3.632 ± 0.003
330.95	1.421 ± 0.002	1.72 ± 0.01	4.203 ± 0.004

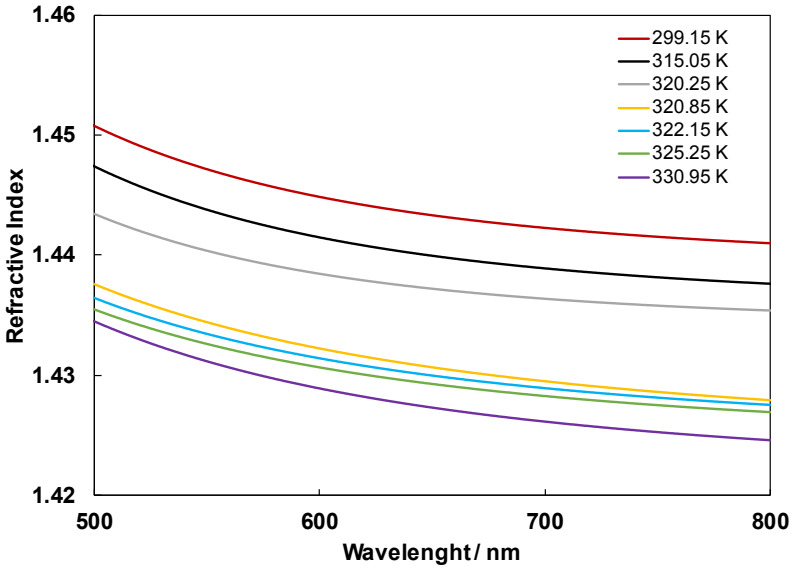

Figure S5. Thermal dependence of the dispersion curves of [$C_{12}C_1$im][BF_4] ILC.

Simulation Details

The [$C_{12}C_1$im][BF_4] ionic liquid was modelled using the CL&P forcefield,[3] and the molecular dynamics simulations were performed and analysed using the Gromacs 5.0.7 software.[4] The equations of motion were solved in 2 fs timesteps using the leap-frog algorithm, and the temperature was controlled with the velocity rescaling algorithm, a weak-coupling thermostat with a stochastic term that ensures the correct canonical ensemble kinetic energy distribution.[5] A 16 Å cut-off was applied to both the electrostatic and dispersive interactions, while both types of interaction beyond the cut-off were treated using the Particle Mesh Ewald method due to the anisotropic nature of the studied systems.

The simulation of the isotropic liquid was started from a random configuration of 1000 ion pairs in a 5 nm x 5nm x 60 nm orthorhombic box with periodic boundary conditions in every direction. It ran in the *NVT* ensemble at 600K, forming an approximately 30 nm thick film with two explicit liquid-vapour (vacuum) interfaces perpendicular to the *zz* axis. After equilibration, confirmed by the constancy of all components of the potential energy, the system was simulated for a further 20 ns and the coordinates were stored every 2 ps for analysis. The density profile was obtained, and it was verified that both interfaces were essentially equal and did not vary with the simulation time.

The liquid crystal phase was started from a 128 ion pair configuration, as described in Bruce *et al.*,[6] which was replicated three times in the direction perpendicular to the smectic planes, generating a system with a total of 384 ion pairs. The obtained triclinic simulation box was then extended in the same direction, generating two explicit interfaces with the vapour (vacuum) phase, with the cation alkyl tails at the interface oriented towards the vacuum. The thickness of the vacuum layer was chosen in order to ensure negligible interactions between the periodic images of the system in the direction perpendicular to the interfaces. This phase was simulated in the *NVT* ensemble at 500 K for 6 ns, the last 5 ns of which were considered for analysis of the structure.

The same initial configuration of the liquid crystal phase was also subjected to a temperature annealing ramp from 500 K to 300 K during 2 ns, and further simulated for 6 ns at 300 K to generate the frozen low-temperature structure (Fig.7 (bottom) and Fig.8). The structure analysis was performed on the last 2 ns of the run. This procedure was performed in the *NpT* ensemble using a fully anisotropic Parrinello-Rahman barostat at null pressure, in order to allow for the increase in density and for eventual changes in the equilibrium unit cell geometry upon cooling.

References

1 C. M. S. S. Neves, K. A. Kurnia, J. A. P. Coutinho, I. M. Marrucho, J. N. C. Lopes, M. G. Freire and L. P. N. Rebelo, Systematic Study of the Thermophysical Properties of Imidazolium-Based Ionic Liquids with Cyano-Functionalized Anions, *J. Phys. Chem. B*, 2013, **177**, 10271–10283.

2 M. A. A. Rocha, C. M. S. S. Neves, M. G. Freire, O. Russina, A. Triolo, J. A. P. Coutinho and L. M. N. B. F. Santos, Alkylimidazolium Based Ionic Liquids: Impact of Cation Symmetry on their Nanoscale Structural Organization, *J. Phys. Chem. B*, 2013, **117**, 10889–10897.

3 J. Canongia Lopes and A. H. Pádua, CL&P: A generic and systematic force field for ionic liquids modeling, *Theor. Chem. Acc.*, 2012, **131**, 1–11.

4 D. Van Der Spoel, E. Lindahl, B. Hess, G. Groenhof, A. E. Mark and H. J. C. Berendsen, GROMACS: Fast, flexible, and free, *J. Comput. Chem.*, 2005, **26**, 1701–1718.

5 G. Bussi, D. Donadio and M. Parrinello, Canonical sampling through velocity rescaling, *J. Chem. Phys.*, 2007, **126**, 014101.

6 D. W. Bruce, Y. Gao, J. N. Canongia Lopes, K. Shimizu and J. M. Slattery, Liquid-Crystalline Ionic Liquids as Ordered Reaction Media for the Diels-Alder Reaction, *Chem. - A Eur. J.*, 2016, **22**, 16113–16123.